Full Paper

Applied Organometallic Chemistry

Received: 11 April 2012 Revised: 7 July 2012 Accepted: 7 July 2012 Published online in Wiley Online Library: 4 October 2012

(wileyonlinelibrary.com) DOI 10.1002/aoc.2905

Two heptadentate Co(III) and Mn(III) complexes with partially deprotonated cyclen derivative bearing four hydroxypropyl pendants: structure, DNA binding and DNA cleavage

Yu-Xin Yin[a,b], Jing-Han Wen[a], Zhi-Rong Geng[a], Yi-Zhi Li[a] and Zhi-Lin Wang[a]*

Two new complexes, $(Co^{III})_2(H_3L^-)_2(0.5H_2O)_2(ClO_4)_4$ (I) and $(Mn^{III})_2(H_3L^-)_2(0.5H_2O)_2(ClO_4)_4$ (II), were synthesized and crystallographically characterized [H_4L = 1,4,7,10-tetra-(2-hydroxypropyl)-l,4,7,10-tetraazacyclododecane] using electrospray ionization mass spectrometry and X-ray photoelectron spectrometery. The characterizations confirmed that the valences of the metal ions increased from divalent to trivalent due to deprotonation of one OH group (H_4L was in the form of H_3L^-). Owing to the instability of Co(III) and Mn(III) in both air and in solution, they preferred to exist in divalent form. The two heptadentate complexes are extraordinary in that the chiral pendants of the complexes are different in configuration. Spectroscopic studies, viscosity measurements, thermal denaturation experiments and circular dichroism spectra demonstrated that the complexes were prone to interact with DNA by groove binding. At micromolar concentrations and under physiological conditions, the two complexes were able to oxidatively cleave the supercoiled pUC19 plasmid DNA into its nicked and linear forms. Mechanistic studies using various additives suggest the complexes had structures different from those of other inorganic complexes. These are the first reported inorganic complexes not containing planar aromatic ligands and yet binding at the major groove.

Supporting information may be found in the online version of this article.

Keywords: 1,4,7,10-tetra-(2-hydroxypropyl)-l,4,7,10-tetraazacyclododecane; Co(III) complex; Mn(III) complex; crystal structure; DNA binding; oxidative cleavage DNA

Introduction

Artificial nucleic acid cleavage agents have attracted extensive attention for their potential applications in the fields of molecular biological technology and drug development.[1–4] The transition metal complexes of macrocyclic polyamines can cleave nucleic acids efficiently, as has been shown in many studies.[5,6] Macrocyclic polyamines with potentially coordinating pendants can form very stable complexes with a wide range of transition metal ions. Ligands encapsulate metal ions in macrocyclic cavities, and the complexes often show excellent thermodynamic and kinetic stability. This is essential for *in vivo* applications.[7–9] Specifically, many ligands based upon the cyclen (12-membered tetraazamacrocycle cyclen (1,4,7,10-tetraazacyclododecane)) containing different types and numbers of pendants have been the subject of intense study.[9,10] Xiao-Qi Yu has synthesized several metal compounds containing cyclen units and evaluated their catalytic abilities on DNA cleavage.[11–13] Thus far, the DNA recognition ability of metal complexes is still not well understood. We believe that the type of coordinated ligand and the geometrical orientation of the ligand are crucial to the binding site specificity and selectivity of a given metal complex.[14] By varying ligands, it is possible to modify the mode of interaction of the complex with nucleic acids and to facilitate individual applications.[15,16] Complexes with unusual coordination numbers and uncoordinated pendants in their stereochemistry may offer an opportunity to explore the effects of coordination geometries on the binding event and to modify the mode of interaction of the complex and DNA.

Cobalt and manganese are essential trace elements in humans, exhibiting many useful biological functions. Numerous compounds, both naturally occurring and man-made, contain cobalt in two common oxidation states: Co(II) and Co(III). In biological reactions manganese can participate in redox reactions by flipping its +2, +3 and +4 oxidation states. There is growing interest in investigating cobalt[17–19] and manganese[20–22] complexes for their interaction with DNA. Among the less studied systems, cobalt(II) and cobalt(III) complexes of polypyridyl ligands, bleomycin, mustard ligands, terpyridine ligands and Schiff bases have been found to efficiently cleave DNA photolytically.[19] Several ligands such as salen, phenanthroline, oxime, cyanonitrosyl and quercetin

* *Correspondence to: Z.-L. Wang, State Key Laboratory of Coordination Chemistry, School of Chemistry and Chemical Engineering, Nanjing University, Nanjing 210093, People's Republic of China. E-mail: wangzl@nju.edu.cn*

[a] *State Key Laboratory of Coordination Chemistry, School of Chemistry and Chemical Engineering, Nanjing University, Nanjing, People's Republic of China*

[b] *School of Chemical Engineering and Materials, Dalian Polytechnic University, Dalian, People's Republic of China*

have been used in the synthesis of manganese-based artificial nucleases.[23] In our work, the THP ligand (THP = H_4L), which contains -OH ligators as shown in Scheme 1(a), was here investigated. This is because it may behave as either an alcohol or an alkoxide donor depending on its deprotonation status.[24] The two heptadentate complexes are unusual in that only three pendants coordinate with the metal ion yet the other pendant does not, as shown in Scheme 1(b). Four pendants in the crystal structure were found to be different chiral structures, and the valences of the metal ion changed from divalent to trivalent due to deprotonation of one -OH group. The calf thymus DNA binding behavior of the two complexes has been investigated through spectroscopic studies, viscosity measurements and thermal denaturation studies. The plasmid pUC19 DNA cleaving behavior of the two complexes has been assessed via agarose gel electrophoresis. We demonstrate that the complexes can bind to DNA via groove binding and effectively promote the cleavage of plasmid DNA via an oxidative pathway.

Results and Discussion

Electrospray Ionization Mass Spectrometry (ESI-MS) and X-Ray Photoelectron Spectrometery (XPS)

The THP ligand, which contains -OH ligators, is interesting because it can form complexes in which the OH can remain protonated and act as an alcohol or can deprotonate and act as an alkoxide.[24,25] Mass spectrometry in the ESI-positive mode in CH_3OH was able to demonstrate the nuclearity of **I** and **II**.[26] It also provided identification on the metal centers. The calculated monoisotopic molecular mass of THP and Co ion is 463.3 Da. There was practically no indication of ligand fragmentation in the spectra. Only two molecular ion peaks centered at *m/z* 462.42 (100%) and *m/z* 231.92 (14%) for complex I confirm the formulation $[Co^{2+} + H_3L^-]^+$ and $[Co^{3+} + H_3L^-]^{2+}/2$ with the deprotonated ligand, as shown in Fig. S1a (supporting information). The calculated monoisotopic molecular mass of THP and Mn ion is 459.3 Da. Complex **II** exhibits two intense peaks centered at *m/z* 229.83(100%) and 458.42 (55%), corresponding to $[Mn^{3+} + H_3L^-]^{2+}/2$ and $[Mn^{2+} + H_3L^-]^+$ ions, respectively, as shown in Fig. S1b (supporting information). ESI-MS observations indicate that the metal-ligated skeletons of these complexes are stable in solution and the perchlorate ligand may dissociate from the complexes. It can be concluded that the valence of the metal ions increases from divalent to trivalent due to deprotonation of one OH group of the THP ligand (i.e. H_4L changed into H_3L^-). Peacock *et al.* have reported that the structure of the Co(III) and Mn(III) complexes with L H_3 (L H_3 = N,N ,N -tris[2-hydroxypropyl]-l,4,7-triazacyclononane) are very similar to the ligand of THP, which occurs as a hydrogen-bridged dimer $[Co(L H_3)(L)Co]^{3+}$ and $[Mn(L H_3)(L)Mn]^{3+}$.[27,28] Under mildly basic conditions (water at pH 7 is sufficient), every second mole of ligand L H_3 deprotonates, and aerial oxidation produces the mixed valence dimer $[M(L H_3)(L)M]^{3+}$. In our experiment, the MeOH solution (H_4L and $Co(ClO_4)_2[Mn(ClO_4)_2]$) was not altered by other alkaline substances. For complex I, the mixed solution was pink on the first day, turning to reddish-brown and precipitating crystals over time. The solution of complex **II** was colorless. After 3 days, the solution and crystals changed to faint yellow. This demonstrated that the oxidation of metal and deprotonation of H_4L are slow and co-instantaneous.

To confirm the valence of the metal ions again, the X-ray photoelectron spectra of the crystals were examined. In these spectra, each major peak can be attributed to a given element or compound. There are no extraneous elements in the spectra, as shown in Figs S2 and S3 (supporting information). For complex I, the peaks of Co(2p3/2) are at about 780.73 and 781.92 eV.[29] The spectral envelope and peak positions can be reproduced by superposition of CoO and CoOOH.[30] The Co(3 s) line at 103 eV was a narrow singlet, with no evidence of the satellite structure identified as a uniquely Co(III) oxide species.[31] For complex **II**, Mn(2p3/2) and Mn(2p1/2) are relatively insensitive to the valency states of Mn.[32] Two peaks for Mn(2p3/2) indicated obviously two valences of metal ion.[33–35] The XPS results can provide additional evidence supporting the valence of the cobalt ions and manganese ions as measured by ESI-MS. Combined with the crystal structure data, it can be confirmed that the metal ions are all trivalent ions in the crystal structure. Mixtures of divalent and trivalent metal ions were observed under ESI-MS and XPS due to the fact that trivalent cobalt and manganese ions are unstable in air and solution. Some of the trivalent metal ions will be slowly reduced to divalent ions. Therefore the two isomorphous complexes that we obtained were $(Co^{III})_2(H_3L^-)_2(0.5H_2O)_2(ClO_4)_4$ and $(Mn^{III})_2(H_3L^-)_2(0.5H_2O)_2(ClO_4)_4$.

Crystal Structure of $(Co^{III})_2(H_3L^-)_2(0.5H_2O)_2(ClO_4)_4$ (I) and $(Mn^{III})_2(H_3L^-)_2(0.5H_2O)_2$ $(ClO_4)_4$ (II)

The structures of the two isomorphous complexes consist of two discrete monomer $[MH_3L^-]^{2+}$ cations, four uncoordinated perchlorate anions and one water molecule each. The two crystallographically independent cations are diastereomers of

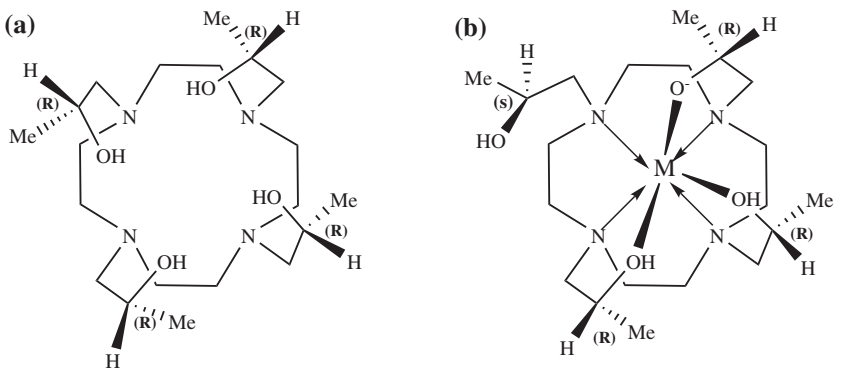

Scheme 1. Schematic structure of the ligand(H_4L) and $[MH_3L]^{2+}$ cation

one another. The pendent hydroxypropyl groups are orientated around the Mn(III) and Co(III) ions in a propeller-like manner in either a clockwise or a counterclockwise direction. The macrocyclic ring can adopt two different conformations when it is coordinated to the metal cation. These two conformations are related by an inversion center. Coupled together, these two structural features give rise to a total of four possible isomers in the crystal structure: the two diastereomers which are present in the defined asymmetric unit and their enantiomeric equivalents. In summary, each crystal of $(Co^{III})_2(H_3L^-)_2(0.5H_2O)_2(ClO_4)_4$ (**I**) and $(Mn^{III})_2(H_3L^-)_2(0.5H_2O)_2$ $(ClO_4)_4$ (**II**) contains four different isomers of the metal (III)-containing cation. The essential atomic labeling scheme for the Co^{3+} cations is given in Fig. 1. Each Co^{3+} cation projecting onto the plane of the four nitrogen atoms in the macrocyclic ring is shown in Fig. 2. The selected bond lengths and angles are listed in Tables 1 and 2.

The $[MH_3L^-]^{2+}$ cations are hepta-coordinated by the four nitrogen atoms of the cyclen (N(1), N(2), N(3), and N(4) or N(5), N(6), N(7) and N(8)), and three oxygen atoms of the hydroxypropyl groups [O(2), O(3) and O(4), or O(6), O(7) and O(8)], and the metal ions are placed in the macrocyclic cavity. The structure of two monomer $[MH_3L]^{2+}$ ions which named the moiety of Co(1)[Mn(1)] ion and the moiety of Co(2)[Mn(2)] ion are very similar. O(4) of the moiety of the Co(1)[Mn(1)] ion and O(8) of the moiety of the Co(2)[Mn(2)] ion have deprotonated their H protons, so they do not form hydrogen bonds with other atoms in the crystal. The geometry is best described as a square prism with one missing vertex, in which four nitrogens of the cyclen form one plane and hydroxypropyl oxygens form the other, with a vacant donor site.[36,37] The chiral pendants of the complexes are not same configuration. The configurations of the coordinated pendants are *R* in the Co(1)[Mn(1)] ion or *S* in the Co(2)[Mn(2)] ion, whereas that of the uncoordinated pendant is *S* in the Co(1)[Mn(1)] ion or *R* in the Co(2)[Mn(2)] ion. The distances of Co(Mn)–O and Co

Table 1. Selected bond lengths (Å) and angles (°) for the Co(III) ion environment of I

Co(1)–O(2)	2.197(2)	Co(2)–O(6)	2.227(2)
Co(1)–O(3)	2.202(2)	Co(2)–O(7)	2.322(2)
Co(1)–O(4)	2.292(2)	Co(2)–O(8)	2.211(2)
Co(1)–N(1)	2.308(3)	Co(2)–N(5)	2.283(3)
Co(1)–N(2)	2.254(3)	Co(2)–N(6)	2.246(3)
Co(1)–N(3)	2.291(3)	Co(2)–N(7)	2.286(3)
Co(1)–N(4)	2.199(3)	Co(2)–N(8)	2.270(3)
O(2)–Co(1)–O(3)	76.19(9)	O(6)–Co(2)–O(7)	80.82(9)
O(3)–Co(1)–O(4)	74.54(9)	O(8)–Co(2)–O(7)	74.55(9)
O(2)–Co(1)–O(4)	81.31(9)	O(8)–Co(2)–O(6)	80.32(9)
N(2)–Co(1)–N(1)	77.04(10)	N(6)–Co(2)–N(5)	77.41(11)
N(2)–Co(1)–N(3)	77.98(10)	N(6)–Co(2)–N(7)	79.06(11)
N(4)–Co(1)–N(3)	78.51(11)	N(8)–Co(2)–N(7)	75.35(11)
N(4)–Co(1)–N(1)	79.95(10)	N(8)–Co(2)–N(5)	79.89(11)

Table 2. Selected bond lengths (Å) and angles (°) for the Mn(III) ion environment of II

Mn(1)–O(2)	2.213(2)	Mn(2)–O(6)	2.2440(2)
Mn(1)–O(3)	2.213(2)	Mn(2)–O(7)	2.328(2)
Mn(1)–O(4)	2.301(2)	Mn(2)–O(8)	2.219(2)
Mn(1)–N(1)	2.321(3)	Mn(2)–N(5)	2.300(2)
Mn(1)–N(2)	2.271(2)	Mn(2)–N(6)	2.254(3)
Mn(1)–N(3)	2.304(3)	Mn(2)–N(7)	2.306(3)
Mn(1)–N(4)	2.217(2)	Mn(2)–N(8)	2.288(2)
O(3)–Mn(1)–O(2)	76.27(8)	O(6)–Mn(2)–O(7)	80.95(8)
O(3)–Mn(1)–O(4)	74.38(8)	O(8)–Mn(2)–O(7)	74.94(8)
O(2)–Mn(1)–O(4)	81.68(8)	O(8)–Mn(2)–O(6)	80.44(8)
N(2)–Mn(1)–N(1)	76.67(9)	N(6)–Mn(2)–N(5)	77.35(10)
N(2)–Mn(1)–N(3)	78.04(9)	N(6)–Mn(2)–N(7)	78.94(10)
N(4)–Mn(1)–N(3)	78.13(10)	N(8)–Mn(2)–N(7)	75.33(10)
N(4)–Mn(1)–N(1)	80.02(9)	N(8)–Mn(2)–N(5)	79.65(10)

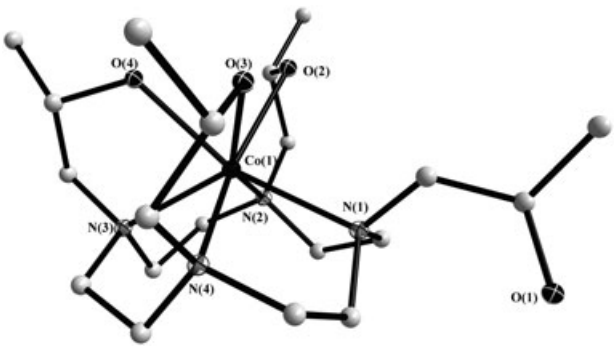

Figure 1. General view of the structure of $[CoH_3L]^{2+}$ cation [Co(1) ion].

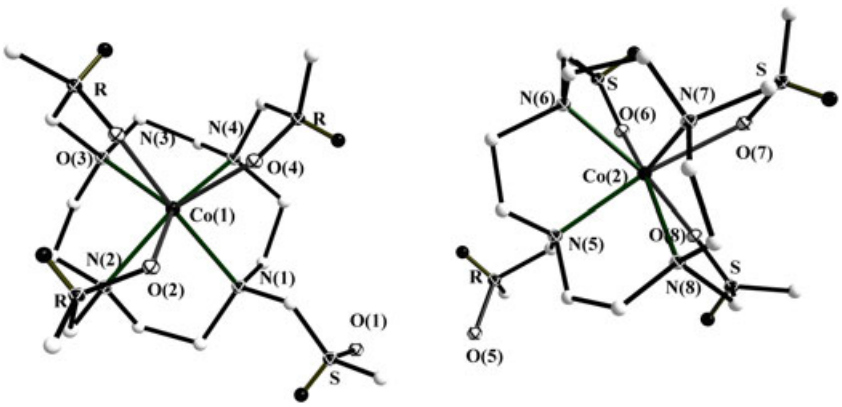

Figure 2. Side-by-side comparison of the two Co(III) cations which define the asymmetric unit.

(Mn)–N vary from 2.197 to 2.328 Å. A basal least-squares plane from the four nitrogens of the cyclen gives a mean deviation of only about 0.0222 Å, while the three oxygen atoms of the hydroxypropyl groups form the other basal face. These two planes form a dihedral angle of about 1.17° and are essentially parallel to each other. The Co(III)[(MnIII)] ion of the moiety of Co(1)[Mn(1)] is displaced by 1.0146(1.0279) Å and 1.5415(1.5484) Å from those two planes. The Co(III)[(MnIII)] ion of the moiety of Co(2)[Mn(2)] is displaced by 1.0383(1.0500) Å and 1.5337(1.5373)Å from those two planes, respectively.

An X-ray crystallographic study of two complexes showed that the perchlorate ions are remote from the molecular cavity. There are four perchlorate anions in the two crystals. Three of them are connected to the ligand by hydrogen bonds. O(32) and O(33) of the perchlorate anion are the acceptors in two single hydrogen bonds from O(2) and O(3) of the moiety of Co(1)[Mn(1)] ion, respectively. The O(22) of the other perchlorate anion is the acceptor for two hydrogen bonds, one each from O(6) and O(7) of the moiety of the Co(2)[Mn(2)] ion. The distances of O(2)–O(32), O(3)–O(33), O(6)–O(22) and O(7)–O(22) are 2.875, 2.930, 2.679 and 2.899 Å, respectively, in complex I. This indicates that the hydrogen bonding is relatively strong. Another uncoordinated oxygen atom (O5) of the Co(2)[Mn(2)] ion forms a hydrogen bond with the uncoordinated oxygen atom (O(1)) of the Co(1)[Mn(1)] ion, which also binds to O(41) of the third perchlorate ion. The O(5)–O(1) and O(5)–O(41) distances are 2.725 and 2.729 Å in complex I. (Hydrogen-bonding distances and angles of the complex I are listed in Table S1 and a perspective view of complex I is shown in Fig. S4 (supporting information)). The O(4) of the Co(1)[Mn(1)] ion moiety and O(8) of the Co(2)[Mn(2)] ion moiety deprotonated their H protons. They do not form hydrogen bonds with other atoms.

Two unexpected heptadentate cobalt(III) and manganese(III) complexes formed by THP of a potential eight-coordinate ligand owing to the increased steric crowding.[38] Until now, the coordinating numbers of the complexes formed by metal ions such as Na(I),[39] Cd(II),[40] Pb(II)[41] and Bi(III)[42] formed by THP was always eight. As the increase of ion radius increases, the distance between the metal ion and the basal plane of the cyclen N atoms increases from 1.0146 to 1.6293 Å. The mean distance of metal ions with coordinated N atoms and O atoms increases from 2.263 to 2.641 Å and from 2.230 to 2.759 Å, respectively, as shown in Table S2 (supporting information). This shows that steric crowding associated with the decreasing ion radius causes the conformation of the two heptadentate complexes.

Thermal Analysis

A crystalline sample, from the same batch used for the crystal structure determination, was subjected to thermogravimetric analysis (TGA). The thermal behavior of the complexes was observed up to 800 °C in a nitrogen atmosphere (Fig. S5 (supporting information)). The TG curves of complexes **I** and **II** showed a homologous three-stage decomposition process from 25 to 440 °C and indicate that the two complexes have analogical thermal stability due to their isomorphic structures. The first loss of weight was accompanied by the loss of all solvent water molecules in the temperature range of 25–250 °C for complexes **I** and **II**. The framework completely collapsed with the decomposition of the H_3L^- ligands and perchlorate anions at the second and the third weight loss stages. TGA showed that the complexes and the framework of the metal ion with the THP exhibit thermodynamic stabilities.

Solution Properties of I and II

Complexes **I** and **II** were highly soluble in water, methanol, ethanol and acetonitrile. The species distributions of **I** and **II** in methanol solution were measured using the ESI-MS method. ESI-MS observations indicated that the metal-ligated skeletons of these complexes were stable in solution and the perchlorate ligand was able to dissociate from the complexes. This suggests that the complexes could covalently bind to DNA after losing the labile perchlorate from ESI-MS.[43]

DNA Binding

DNA binding is the critical step for DNA activity. Therefore, the ability of the complexes to bind calf thymus (CT) DNA was studied by using UV–visible absorption, viscosity measurements, thermal denaturation and fluorescence spectroscopy.

Electronic absorption spectroscopy is universally employed to determine the binding characteristics of metal complex with DNA. The absorption spectra of the two complexes in the absence and presence of calf thymus DNA are shown in Fig. 3. The intensity changes in the intraligand π–π* transition band at 204.2 and 211.4 nm, which is attributed to the ligand-to-metal charge transfer absorption. The value of the intrinsic binding constants K_b (5×10^3 M^{-1}for **I** and 2×10^3 M^{-1} for **II**) were determined by regression analysis using equation (1). The K_b values were much smaller than those reported for typical classical intercalators (10^7 M^{-1}).[44–46] Because the complexes do not contain any

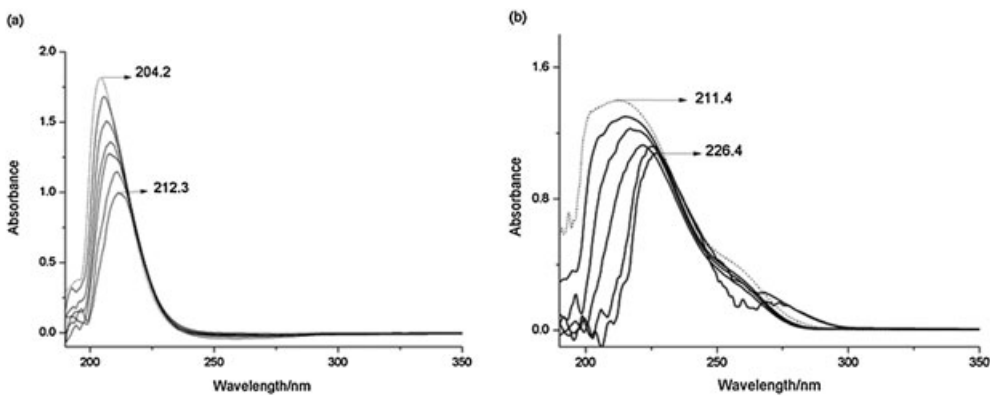

Figure 3. Absorption spectra of complexes **I** (a) (1.67×10^{-3} M) and **II** (b) (4.4×10^{-5} M) in the absence (dashed line) and presence (solid line) of increasing amounts of CT DNA (0–2.7×10^{-4} M of **I** and 0–2.36×10^{-4} M of **II**) at room temperature in 5 mM Tris–HCl/NaCl buffer (pH 7.2). The dashed lines indicate the free complexes.

fused aromatic rings to facilitate intercalation, classical intercalative interaction might be impossible.[47–49] We determined that complexes **I** and **II** more likely bind to DNA by groove (surface) binding.[47–50]

Spectroscopic techniques are used to study the binding model of metal complexes with DNA, but they do not give sufficient information to support a binding model. Hydrodynamic measurements, which are very sensitive to changes in the length of the DNA, are the least ambiguous and the most decisive tests of the binding model of metal complexes with DNA in solution. In the absence of crystallographic structural data for metal complexes, these viscosity measurements are taken to be the most convincing tests for the binding modes of the metal complexes with DNA. In the intercalation model, DNA base pairs are elongated so as to accommodate the binding ligand, thereby increasing the viscosity of DNA. In contrast, a partial or non-classical intercalation of ligand can bend or kink the DNA helix, reduce its effective length and therefore reduce concomitantly viscosity.[51–55] In the presence of complexes **I** and **II**, DNA viscosity has been found to decrease. The decrease in viscosity suggests that the complex can bind to DNA not by the classical intercalation binding mode but by external contact (surface binding) or groove binding, as shown in Fig. 4.[50,56] The results of the viscosity experiments confirm the groove mode of binding of these complexes through absorption spectral studies.

Thermal behavior of DNA in the presence of metal complexes can provide information regarding the strength of interaction between those complexes and DNA. When the temperature of the solution is gradually increased, the double-stranded DNA dissociates into single-stranded, producing changes in the absorption intensity at the 260 nm wavelength. In order to evaluate this transition process, the melting temperature (T_m), defined as the temperature at which half of the polynucleotide strands have denatured from double-stranded to single-stranded, is a valuable parameter. A high ΔT_m value suggests an intercalative binding mode of the metal complex to DNA, while a low value (1–3 °C) indicates a non-intercalative binding mode.[57,58] The melting curves of CT DNA in the absence and presence of both the complexes are presented in Fig. 5. The melting temperature of double-helical CT DNA under the present experimental conditions was found to be about 78.4 °C.[51] This temperature corresponds to the breaking of hydrogen bonds between the base pairs present in the double-stranded DNA to form the single-stranded DNA structure. With the addition of complexes **I** and **II**, T_m increased to about 80.0 °C and 81.5 °C, respectively, at a concentration ratio of metal complex to DNA of 1:2. The

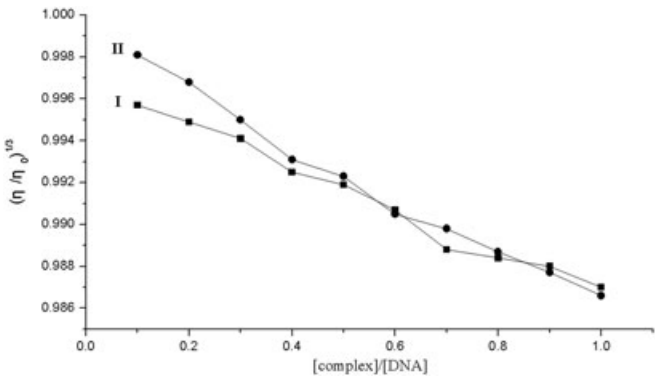

Figure 4. Effect of increasing amounts of the complexes on the relative viscosity of CT DNA at 30.0 ± 0.1 °C.

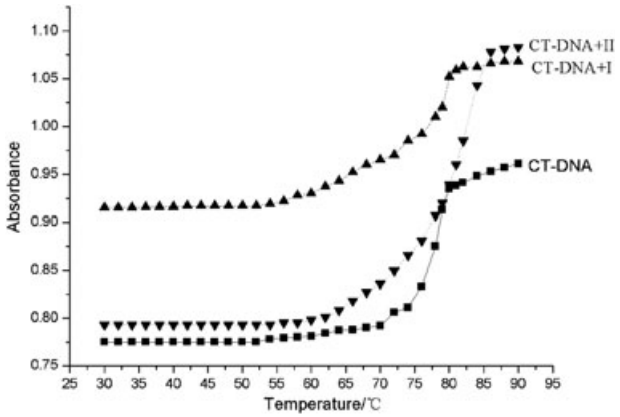

Figure 5. Derivative plot of DNA melting for CT DNA (170 mM) in the absence and presence of complexes **I** and **II**. The inset shows the corresponding melting curves for the DNA duplex in the absence (squares) and presence of complexes **I** (▲) and **II** (▼) in 10 mM phosphate buffer (pH 7.2).

ΔT_m values of 1.6 °C and 3.1 °C suggest that these complexes bind to DNA through non-intercalative groove binding, as can be determined from the spectroscopic titration.[51,56]

The competitive binding of the two complexes with CT DNA was here investigated using a fluorescence spectral method. Measurements were carried out using the emission intensity of ethidium bromide (EB) bound to DNA as a probe. EB emits intense fluorescence in the presence of DNA due to its strong intercalation between the adjacent DNA base pairs. Its displacement from DNA by a metal complex results in a decrease in fluorescence intensity.[59–61] In competitive binding studies, the two complexes were added to CT DNA pretreated with EB and then the emission intensities of DNA-induced EB were measured. The extent to which EB fluorescence was quenched was used to determine the extent of binding between the second molecule and DNA. From the plot of I_0/I and [complex] (I_0 is the emission intensity of EB-DNA in the absence of complex; I is the emission intensity of EB-DNA in the presence of complex) (Fig. 6), the apparent binding constant (K_{app}) values for complexes **I** and **II** are 326 and 117 M^{-1}, respectively. The binding constants of the classical intercalators are of the order of 10^7 M^{-1}.[44] Thus the data

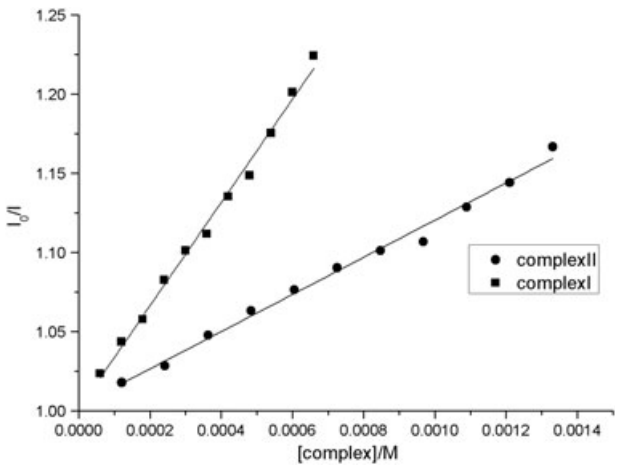

Figure 6. Plot of I_0 /I versus [complex]. Complex **I** (■) and II (·): I_0 is emission intensity of EB DNA in the absence of complex. I is emission intensity of EB DNA in the presence of complex.

are consistent with our hypothesis. The two complexes bind to DNA in groove binding mode.[61]

Circular dichroism (CD) spectroscopy of DNA-type substances is a sensitive technique that gives information on the conformational changes and destabilization of the DNA helix.[62,63] Simple groove binding and electrostatic interaction of small molecules show little or no perturbation on the base-stacking and helicity bands, while intercalation enhances the intensities of both the bands stabilizing the right-handed B conformation of CT DNA. The changes in the positive band at 278 nm can be explained by the alteration of base stacking and the negative band at 245 nm due to the changes of the helicity of B-DNA.[64] The CD spectra of calf thymus DNA after addition of complexes **I** and **II** at ratios of $r = 1$ are shown in Fig. 7. The positive band of CT DNA slight decreased in intensity upon addition of the complexes, indicating that the complexes do not interact with the DNA bases, which is consistent with our conclusion that the two complexes bind to DNA in groove binding mode.[65,66] Meanwhile, the negative band undergoes obvious reductions almost without shift in the band positions.

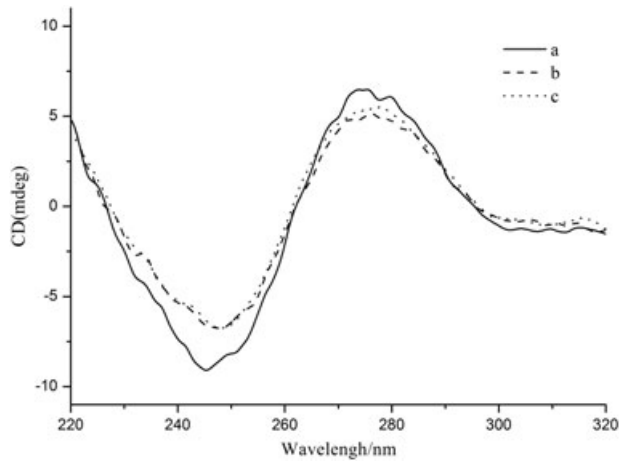

Figure 7. CD spectra of CT DNA in the absence (a) and presence (b) of complex **I** at $r = 1$, and in the presence of complex **II** (c) at $r = 1$. [DNA] = 1.1 mM.

The results suggest that the complexes unwind the DNA helix and lead to some helicity losses.[67–69] DNA remains in the B-type conformation because there is no shift of the band positions.[63] Furthermore, the decreased intensity of DNA helicity band indicates the hydrophobic interaction of -NH- and $-CH_3$ groups with DNA.[66] The covalent binding to DNA of the complexes NAMI and RAP caused similar alterations of the characteristic CD bands of B-type DNA.[69]

DNA Cleavage

The nuclease activity of complexes **I** and **II** were studied using supercoiled (SC) pUC19 DNA in a medium of 4-(2-hydroxyethyl)-1-piperazineethanesulfonic acid (HEPES) buffer (pH 7.2). Under anaerobic conditions, complexes **I** and **II** did not cleave DNA (Fig. S6 (supporting information). This implies that the DNA cleavage reaction of complexes **I** and **II** has an oxidative mechanism.[44]

Incubation of pUC19 DNA (18 μM) with complexes **I** and **II** at pH 7.2 for 2 h at 37 °C resulted in an extensive cleavage of DNA. This increased remarkably with the concentration of metal complex, reaching a maximum at approximately 6 μM complexes **I** and **II** in the presence of H_2O_2. It then decreased as shown in Fig. S7 (supporting information). We also investigated the DNA cleavage reaction by examining complexes without H_2O_2, as shown in Fig. S8 (supporting information). The results were similar to those of the reaction in the presence of H_2O_2. A comparison of the reactivity at equivalent ion concentrations showed that reactivity in the absence of H_2O_2 was considerably higher than in the presence of H_2O_2. The activity of cleaving DNA for complexes **I** and **II** increased with concentrations of complexes **I** and **II**, up to a maximum at approximately 5 and 4 μM, respectively. The comparably fast decrease that followed suggests the concentration-dependent formation of an unreactive species. Similar behavior has been reported for plasmid DNA. This has been attributed to the formation of unreactive μ-hydroxo dimers that may compete with the reactive monomeric complexes for the binding.[70,71] The time dependence of the cleavage reaction by complexes **I** and **II** was examined in the presence of H_2O_2 at the optimal complex concentration of 6 μM (Fig. 8). The reaction

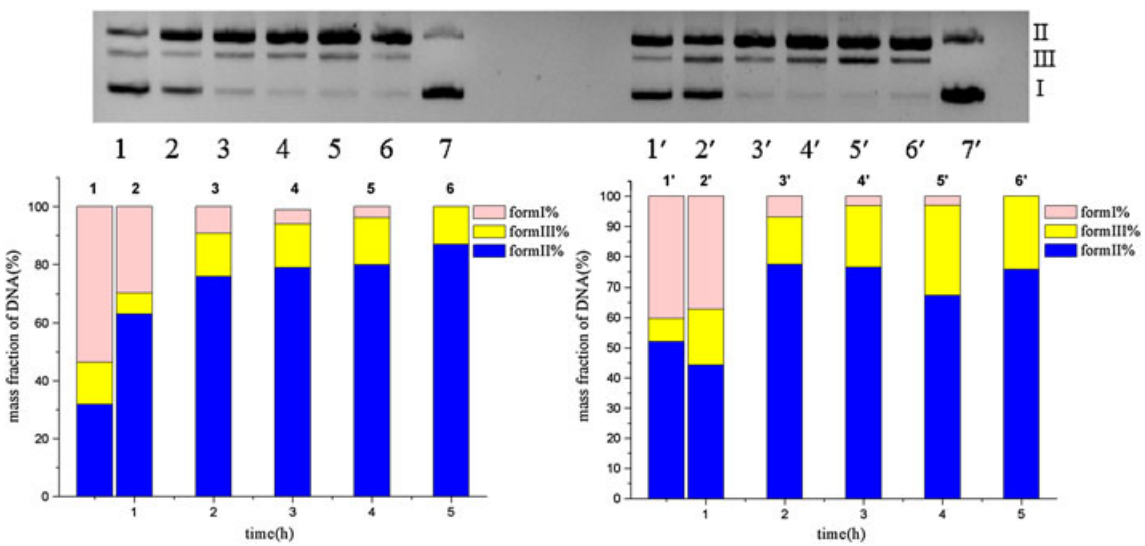

Figure 8. Agarose gel electrophoresis diagrams and corresponding histograms showing cleavage of SC pUC19 DNA by complex **I** (**II**). Time course of conditions: 18 μM DNA; 6 μM complex **I** (**II**); 0.1 mM H2O2; 10 mM HEPES buffer; pH 7.2; 37 °C; lane 1 (1): 0.5 h; lane 2 (2): 1 h; lane 3 (3): 2 h; lane 4 (4): 3 h; lane 5 (5): 4 h; lane 6 (6): 5 h; lane 7 (7): DNA control.

was monitored for 5 h. Extensive cleavage of DNA was observed for the complexes, with most of the supercoiled DNA consumed within 2 h. Complex **I** (**II**) cleaved the SC form (form I) to 91% (93%), producing 76% (78%) nicked circular form (form II) and 15% (16%) linear form (form III) (lane 3 (3) (Fig. 8), respectively. Although the reaction velocity constant was not calculated, their efficiencies of oxidative cleavage of DNA were obvious. They were not worse than hydrolytic or oxidative cleavage agents in other systems from the reaction time and concentration of the complexes.[36,72–74]

The DNA cleavage mechanisms of complexes **I** and **II** were investigated in the presence of hydroxyl radical scavengers (DMSO, EtOH), singlet oxygen quenchers (L-histidine, NaN_3), and a superoxide ion scavenger (KI) under aerobic conditions, as shown in Fig. S9 (supporting information). The DNA cleavage mechanism of complexes **I** and **II** is illustrated as follows. KI is nearly ineffective, which rules out the possibility that DNA could be cleaved by hydroxyl superoxide ion. The addition of L-histidine and DMSO was found to sufficiently inhibit the activity of the two complexes in a way similar to nuclease. This implies that the singlet oxygen and hydroxyl radicals play key roles in cleavage chemistry.[75,76] To determine whether those complexes preferentially bound at the DNA groove, DNA cleavage experiments were carried out in the presence of a major groove binder (methyl green) and a minor groove binder (distamycin), as shown in Fig. 9. Distamycin did not seem to inhibit the cleavage of complex **I** or **II**. Rather, this shows strong facilitating effects, especially for complex **II**. Methyl green was found to inhibit cleavage of the two complexes, especially complex **I**, which showed almost no reaction with DNA in the presence of methyl green. These results show that the complexes prefer the major groove binding.[75,76] The metal-ligated skeletons of the two complexes are stable in solution, as shown in Fig. S10 (supporting information). The structures of the complexes are composed of two cuboids. The length, height and width of one cuboid are 4.88 (4.89), 2.69 (2.71) and 4.256 (4.279) Å, and those of the other are 4.66 (4.67), 4.6 (4.5) and 7.45 (7.5) Å. The total length of the two cuboids is 9.54 (9.56) Å. The major groove width and depth of the B-DNA are 11.7 and 8.5 Å, and the minor grooves are 5.7 and 7.5 Å.[77] Although the length of the cuboids is slightly longer than the depth of the B-DNA, the height (4.66 (4.67) Å) and width (7.45 (7.5) Å) of the complexes are both shorter than the width of the major groove width (11.7 Å). The complexes can pass into the major groove but not into the minor groove. The major groove binding complexes that have been reported by Barton *et al.*[78–80] and Chakravarty *et al.*[81–83] all exhibit rigid or mostly rigid three-dimensional structures, but their mechanism of DNA cleavage is photocleavage in all cases. The only proposed intercalation via the major groove is the dipyridophenazine (dppz) ligand intercalation from the major groove. The metal–phenazine axis lies along the DNA dyad axis or the long axis of the base pairs.[78,81] By comparison with the spatial configuration of their complexes and our own, complexes **I** and **II** do not contain any planar aromatic ligands. They cannot extend into the base stack upon DNA binding. They are the first small, inorganic complexes not containing any planar aromatic ligand but nonetheless showing oxidative cleavage of supercoiled DNA binding at the major groove binding. We speculate that the complexes can enter the major groove, in which the uncoordinated pendant of THP would act as a wedge to bind one side of a base pair stack by the groove binding model.[84] Hydroxyls may form hydrogen bonds and Van der Waals forces with the heterocyclic bases and deoxyribose at the binding site.[85] Therefore, DNA at the binding site becomes easier to be cleave oxidatively because of groove binding via the major groove.

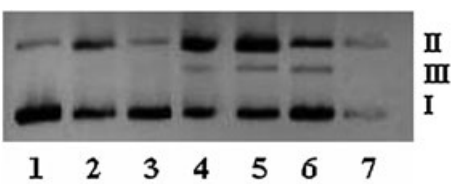

Figure 9. Agarose gel electrophoresis diagrams showing cleavage of SC pUC19 DNA by complex **I** (**II**). Conditions: 18 μM DNA; 10 μM complex **I** (**II**); 0.1 mM H2O2; 10 mM HEPES buffer; pH 7.2; 37 °C; incubation time, 2 h; lane 1: DNA control; lane 2: complex **I**; lane 3: complex **I** + 0.02 mM methyl green; lane 4: complex **I** + 0.02 mM distamycin; lane 5: complex **II**; lane 6: complex **II** + 0.02 mM methyl green; lane 7: complex **II** + 0.02 mM distamycin.

Conclusion

The ligand THP has shown considerable selectivity for metal ions of large size.[86,87] The OH of the ligand can be deprotonated, acting as an alkoxide. The deprotonated OH (O^-) of the ligand causes the valence of the metal ion to change from divalent to trivalent, and the radius of Co(III) and Mn(III) cannot match the fixed size of the cavities. This increases steric crowding, which finally results in two asymmetric heptadentate complexes. The spectroscopic studies, viscosity measurements and thermal denaturation studies suggest that the complexes bind to DNA by groove binding. The two complexes cleave the supercoiled pUC19 plasmid DNA into its nicked and linear forms at micromolar concentrations under physiological conditions. The mechanistic study suggests they are the first inorganic complexes not containing planar aromatic ligands to show oxidative cleavage of supercoiled DNA binding at the major groove. The spatial structures of complexes are important for the binding site. This work provides an opportunity to use other 12-membered macrocyclic tetraamine complexes that have uncoordinated pendants that may be designed and functionalized for cleavage of DNA binding at the major groove. Their high cleavage efficiency makes them attractive molecules for therapeutic applications.

Experimental Procedures

CAUTION: although no problems were encountered in the course of this study, transition metal perchlorates are potentially explosive and should therefore be prepared in small quantities and handled with care.

Materials and Methods

All reagents and chemicals were procured from commercial sources and used without further purification. SC pUC19 plasmid DNA (caesium chloride purified) was purchased from TaKaRa Biotechnology (Dalian). CT DNA, agarose (molecular biology grade), tris(hydroxymethyl) aminomethane (Tris), distamycin, methyl green and EB were obtained from Sigma. Milli-Q water was used for the preparation of the buffers.

Elemental analyses (C, H and N) were performed on a vario EL II elemental analyzer. Infrared spectral data were obtained using a Bruker TENOR 27 spectrophotometer. ESI mass spectra were recorded using an LCQ fleet ESI mass spectrometer (Thermo

Scientific). UV–visible spectra were determined on a Shimadzu UV 3600 (UV–visible near-IR) spectrophotometer. Fluorescence spectra were recorded on a PerkinElmer LS55 luminescence spectrometer in a wavelength range of 530–780 nm with 4 nm slits for both excitation and emission at room temperature. Fluorescence imaging was performed with a Gel Doc XR (BioRad), and quantification analysis was performed with Quantity One software (version 4.6.2). Thermogravimetric analyses were performed using a TA Instruments SDT2960 analyzer with a heating rate of 10 °C min^{-1} in a nitrogen atmosphere. Anaerobic conditions were achieved using an MBRAUN LABStar glove box. X-ray photoelectron spectra of crystal samples were obtained using a K-Alpha X-ray photoelectron spectrometer (Thermo Fisher Scientific) with a Al K-Alpha X-ray radiation as the source for excitation with a source energy of 1253.60 eV, pass energy of the spectrometer set at 50 eV, at steps of 0.1 eV.

Synthesis of the Complexes

THP was prepared from racemic propylene oxide and cyclen as reported by Hancock and co-workers, and four chiral centers were introduced into the macrocycle.[86,88] Various combinations of *R* and *S* configurations at the α-C of the pendent hydroxypropyl groups gave rise to possible stereoisomers.

Preparation of $(Co^{III})_2(H_3L^-)_2(0.5H_2O)_2\ (ClO_4)_4$ ***(I)***

The complex was prepared using a general procedure. A solution of $Co(ClO_4)_2.6H_2O$ (0.25 mmol, 91.2 mg) in 5 ml MeOH was added dropwise to a stirred solution of THP (0.25 mmol, 101 mg) in 5 ml MeOH at room temperature. A pink solution was immediately obtained under aerobic conditions. After filtration, a week later, reddish-brown X-ray-quality crystals were obtained by vapor diffusion of Et_2O into a solution of MeOH (yield 58 mg, 30%). Elemental analysis data: Calcd (%) for $C_{40}H_{88}C_{l4}Co_2N_8O_{25}$: C, 35.83; H, 6.62; N, 8.36. Found (%): C, 36.16; H, 6.83; N, 8.27. IR (KBr) cm^{-1}: 3422.2 (OH), 2873.5, 2974.54 (CH), 1092 (ClO_4^-). The complex was identified by ESI-MS in positive mode. The calculated monoisotopic molecular masses were as follows: THP + Co^{2+} equal to 463.3 Da, analytical data: 462.42(100) $[H_3L^- + Co^{2+}]^+$; 231.92(14) $[H_3L^- + Co^{3+}]^{2+}/2$.

Preparation of $(Mn^{III})_2(H_3L^-)_2(0.5H_2O)_2\ (ClO_4)_4$ ***(II)***

The complex was prepared using a method similar to that described for $(Co^{III})_2(H_3L^-)_2\ (0.5H_2O)_2(ClO_4)_4$ (**I**). A colorless solution was obtained, and the solution changed to faint yellow after 3 days. Two weeks later, faint yellow crystals were obtained which were suitable for X-ray analysis (yield 74.8 mg, 35%). Elemental analysis data: Calcd (%) for $C_{40}H_{88}C_{l4}Mn_2N_8O_{25}$: C, 36.05; H, 6.65; N, 8.41. Found (%): C, 36.63; H, 6.94; N, 8.33. IR (KBr) cm^{-1}: 3407.2 (OH), 2974.54, 2865.9 (CH), 1091.6 ($ClO4^-$). The complex was identified by ESI-MS in positive mode. The calculated monoisotopic molecular masses are as follows: THP + Mn^{2+} equal to 459.3 Da, analytical data: 458.42(55) $[H_3L^- + Mn^{2+}]^+$; 229.83(100) $[H_3L^- + Mn^{3+}]^{2+}/2$.

X-Ray Crystallography

Crystal data were collected using a Bruker SMART APEX CCD diffractometer with graphite monochromated Mo *Kα* radiation ($\lambda = 0.71073$ Å) at room temperature. All absorption corrections were performed by using the SADABS program.[89] The structures were solved by direct methods and refined by full-matrix least-squares on F^2 using the SHELXTL-97 program package.[90] All non-hydrogen atoms were located in different Fourier maps and refined anisotropically. All H atoms were placed in geometrically idealized positions and refined isotropically. All the crystallographic parameters are tabulated in Table 3 (CCDC reference numbers 764010 and 764011). These data can be obtained free of charge from the Cambridge Crystallographic Data Centre (www.ccdc.cam.ac.uk/data_request/cif).

DNA Binding Experiments

All experiments involving interaction of the compound with CT DNA were conducted in Tris buffer (5 mM Tris–HCl/NaCl buffer, pH 7.2). The purity of the DNA was determined by monitoring the value A_{260}/A_{280} about 1.8–1.9: 1, indicating that the DNA was sufficiently free of protein.[91] The stock solution of CT DNA was stored at 4 °C and used within 4 days. The DNA concentration per nucleotide was determined by absorption spectroscopy using the molar absorption coefficient (6600 M^{-1} cm^{-1}) at 260 nm.[92] Absorption titration experiments were performed by varying the concentration of CT DNA, keeping the metal complex concentration constant. The same concentration of buffered CT DNA solution was added to each cuvette to eliminate absorption from DNA itself. The binding constant was determined using the following equation:[44]

$$[\mathrm{DNA}]/(\varepsilon_A - \varepsilon_F) = [\mathrm{DNA}]/(\varepsilon_B - \varepsilon_F) + 1/K_b(\varepsilon_B - \varepsilon_F) \qquad (1)$$

Here ε_A, ε_F, and ε_B correspond to A_{obsd}/[complex], the extinction coefficient for the free complex, and the extinction coefficient for the complex in the fully bound form, respectively.

Viscosity experiments were carried out with an Ubbelodhe viscometer, which was immersed in a thermostated water bath maintained at 30 ± 0.1 °C. DNA samples of approximately 0.5 mM were prepared by sonicating in order to minimize complexities arising from DNA flexibility. Flow time was measured with a digital stopwatch. Each sample was measured three times and an average flow time was calculated.[93] The data are presented as $(\eta/\eta_0)^{1/3}$ versus [complex]/[DNA], where η is the viscosity of DNA in the presence of the complex, and η_0 is the viscosity of DNA alone. Viscosity values were calculated from the observed flow time of DNA containing solutions (t) corrected for that of the flow time of the buffer alone (t_0): $\eta = t - t_0/t_0$. DNA melting experiments were carried out by monitoring the absorbance of CT DNA (180 mM NP) at 260 nm at various temperatures in the absence and presence of the two complexes in a 2:1 ratio of the DNA and complex with a ramp rate of 0.5 °C min^{-1} in phosphate buffer medium (pH 7.2) using a Peltier system attached to the UV–visible spectrophotometer. The relative binding of the two complexes to CT DNA was evaluated with an EB-bound CT DNA solution in 5 mM Tris–HCl/NaCl buffer (pH 7.2). Fluorescence intensities at about 603 nm (520 nm excitation) were measured at different complex concentrations. Emission intensity showed a reduction upon addition of the complex. The relative binding propensity of the complexes to CT DNA was determined from the comparison of the slopes of the lines representing fluorescence intensity versus the complex concentration plot. The apparent binding constant (K_{app}) was calculated from the equation $K_{EB}[EB] = K_{app}[complex]$, $K_{EB} = 1.0 \times 10^7$ M^{-1} ([EB] = 4.0 μM).[44] All CD spectroscopic studies were carried out with a continuous flow of nitrogen purging the polarimeter, using a Jasco J-810 automatic recording spectropolarimeter, and the measurements were performed at room temperature with 0.1 cm pathway cells. The CD spectra were run from 320 to 220 nm

Table 3. Crystallographic data for complexes I and II

Empirical formula	$C_{40}H_{88}Cl_4Co_2N_8O_{25}$(I)	$C_{40}H_{88}Cl_4Mn_2N_8O_{25}$(II)
M_r	1340.84	1332.86
T (K)	291(2)	291(2)
Crystal system	Monoclinic	Monoclinic
λ (Å)	0.71073	0.71073
Space group	P2(1)/c	P2(1)/c
a (Å)	15.6124(17)	15.7001(11)
b (Å)	14.2742(15)	14.3914(10)
c (Å)	27.519(3)	27.5946(19)
α, γ (°)	90.00	90.00
B (°)	95.604(2)	95.7940(10)
V (Å^3)	6103.4(11)	6203.0(7)
Z	4	4
D (Mg m^{-3})	1.427	1.459
μ (mm^{-1})	0.660	0.801
F (000)	2808	2824
Crystal size (mm)	0.30 × 0.26 × 0.24	0.30 × 0.26 × 0.24
θ range for data collection (°)	1.88–26.00	1.87–26.00
Limiting indices, hkl	−18 to 19, −17 to 17, −22 to 33	−19 to 13, −16 to 17, −34 to 31
Reflections collected	32 435	33 019
Independent reflections (R(int))	11 980	12 190
Goodness of fit on F^2	1.091	1.068
$R1$/w$R2$ [$I > 2\sigma(I)$]	0.0542/0.1478	0.0543/0.1307
$R1$/w$R2$ (all data)	0.0674/0.1530	0.0734/0.1364
Largest diff. peak (e Å^{-3})	0.614/−0.901	0.677/−0.385

at a speed of 20 nm min^{-1} and the buffer background was automatically subtracted. Data were recorded at intervals of 0.1 nm. The CD spectrum of CT-DNA alone (1.1 mM) was recorded as the control experiment.[67]

DNA Cleavage Experiments

Cleavage of SC pUC19 plasmid DNA by the complexes was evaluated via agarose gel electrophoresis. SC pUC19 plasmid DNA in HEPES buffer (pH 7.2) was treated with the indicated amounts of complex followed by dilution with HEPES buffer to a total volume of 10 μl. The samples were incubated at 37 °C. After the reaction had been stopped by addition of 1/10 volume of the loading buffer (0.25% bromophenol blue, 40% sucrose, 0.25% xylene cyanole and 200 mM ethylenediaminetetraacetic acid (EDTA)), the samples were loaded on 1% neutral agarose gel containing 40 mM Tris–acetate and 1 mM EDTA (TAE buffer, pH 8.0). They were then subjected to electrophoresis in a horizontal slab gel apparatus and 1× TAE buffer, which was run at 75 V for 1.5 h. Agarose gel electrophoresis of plasmid DNA was visualized by photographing the fluorescence of intercalated EB under a UV illuminator. The proportion of DNA in each fraction was estimated quantitatively from the intensity of the bands using Glyko BandScan software. Deoxygenated solutions were prepared by four freeze–pump–thaw cycles. Before the final two cycles, the solutions were equilibrated with argon to aid in the deoxygenation process. The deoxygenated solutions were stored in an argon atmosphere prior to use. Anaerobic conditions were achieved using an MBRAUN LABStar glove box. Solutions of SC pUC19 plasmid DNA, HEPES buffer and the complexes were all kept under anaerobic conditions in a glove box for 3 h before the solutions were mixed. Reaction mixtures were prepared in a glove box by addition of the appropriate volumes of stock solutions to the reaction tubes. They are incubated at room temperature for 3 h and then quenched by addition to the loading buffer in the glove box. All other conditions were the same as those listed for the aerobic cleavage reactions. Cleavage mechanistic investigation of pUC19 DNA was performed using different reagents such as DMSO, L-histidine, KI, NaN_3 and EtOH, which were added to pUC19 DNA prior to the addition of complexes.

Acknowledgements

This work was supported by the National Natural Science Foundation of China (21075064, 21027013, 20721002, and 90813020) and the National Basic Research Program of China (2007CB925102).

References

[1] C. Metcalfe, J. A. Thomas, *Chem. Soc. Rev.* **2003**, *32*, 215.
[2] C. Liu, M. Wang, T. Zhang, H. Sun, *Coord. Chem. Rev.* **2004**, *248*, 147.
[3] J. A. Cowan, *Curr. Opin. Chem. Biol.* **2001**, *5*, 634.
[4] J. R. Morrow, O. Iranzo, *Curr. Opin. Chem. Biol.* **2004**, *8*, 192.
[5] M. Demeunynck, C. Bailly, *Small Molecule DNA and RNA Binders: From Synthesis to Nucleic Acid Complexes*, Wiley-VCH, Weinheim, **2002**.
[6] B. N. Trawick, A. T. Daniher, J. K. Bashkin, *Chem. Rev.* **1998**, *98*, 939.
[7] M. Meyer, V. Dahaoui-Gindrey, C. Lecomte, R. Guilard, *Coord. Chem. Rev.* **1998**, *178–180*, 1313.
[8] S. F. Lincoln, *Coord. Chem. Rev.* **1997**, *166*, 255.
[9] K. P. Wainwright, *Coord. Chem. Rev.* **1997**, *166*, 35.
[10] E. Tfouni, K. Q. Ferreira, F. G. Doro, R. S. Silva, Z. N. Rocha, *Coord. Chem. Rev.* **2005**, *249*, 405.
[11] Q. X. Xiang, J. Zhang, P. Y. Liu, C. Q. Xia, Z. Y. Zhou, R. G. Xie, X. Q. Yu, *J. Inorg. Biochem.* **2005**, *99*, 1661.
[12] W. Peng, P. Y. Liu, N. Jiang, H. H. Lin, G. L. Zhang, X. Q. Yu, *Bioorg. Chem.* **2005**, *33*, 374.
[13] Q. L. Li, J. Huang, Q. Wang, N. Jiang, C. Q. Xia, H. H. Lin, J. Wu, X. Q. Yu, *Bioorg. Med. Chem.* **2006**, *14*, 4151.
[14] L. F. Chin, S. M. Kong, H. L. Seng, K. S. Khoo, R. Vikneswaran, S. G. Teoh, M. Ahmad, S. B. A. Khoo, M. J. Maah, C. H. Ng, *J. Inorg. Biochem.* **2011**, *105*, 339.
[15] S. Liu, D. S. Edwards, *Bioconjugate Chem.* **2001**, *12*, 7.
[16] R. Delgado, V. Felix, L. M. P. Lima, D. W. Priced, *Dalton Trans.* **2007**, 2734.
[17] A. D. Richards, A. Rodger, *Chem. Soc. Rev.* **2007**, *36*, 471.
[18] A. Terrón, J. J. Fiol, A. García-Raso, M. Barceló-Oliver, V. Moreno, *Coord. Chem. Rev.* **2007**, *251*, 1973.
[19] F. R. Keene, J. A. Smith, J. G. Collins, *Coord. Chem. Rev.* **2009**, *253*, 2021.
[20] R. Indumathy, T. Weyhermüller, B. U. Nair, *Dalton Trans.* **2010a**, 2087.
[21] E. D. Mauro, R. Saladino, P. Tagliatesta, V. D. Sanctis, R. J. Negri, *Mol. Biol.* **1998**, *282*, 43.
[22] U. Schatzschneider, *Eur. J. Inorg. Chem.* **2010**, 1451.
[23] L. N. Zhu, Y. W. Jin, X. Z. Li, J. Wang, D. M. Kong, H. F. Mi, D. Z. Liao, H. X. Shen, *Inorg. Chim. Acta* **2008**, *361*, 29.
[24] R. D. Peacock, J. Robb, *Inorg. Chim. Acta* **1986**, *121*, L15.
[25] A. A. Belal, P. Chaudhuri, I. Fallis, L. J. Farruia, R. Hartung, N. M. Macdonald, B. Nuber, R. D. Peacock, J. Weiss, K. Wieghardt, *Inorg. Chem.* **1991a**, *30*, 4397.
[26] V. Pavlishchuk, F. Birkelbach, T. Weyhermüller, K. Wieghardt, P. Chaudhuri, *Inorg. Chem.* **2002**, *41*, 4405.
[27] A. A. Belal, L. J. Farrugia, R. D. Peacock, J. Robb, *J. Chem. Soc. Dalton Trans.* **1989**, 931.
[28] A. A. Belal, P. Chaudhuri, I. Fallis, L. J. Farrugia, R. Hartung, N. M. Macdonald, B. Nuber, R. D. Peacock, J. Weiss, K. Wieghardt, *Inorg. Chem.* **1991b**, *30*, 4397.
[29] Y. Xie, H. H. Wu, G. P. Yong, Z. Y. Wang, R. Fan, R. P. Li, G. Q. Pan, Y. C. Tian, L. S. Sheng, L. Pan, J. Li, *J. Mol. Struct.* **2007**, *833*, 88.
[30] N. S. McIntyre, M. G. Cook, *Anal. Chem.* **1975**, *47*, 2208.
[31] J. C. Dupin, D. Gonbeau, H. Benqlilou-Moudden, P. Vinatier, A. Levasseur, *Thin Solid Films* **2001**, *384*, 23.
[32] L. D. Mishima, T. Ohtsuka, H. Konno, N. Sato, *Electrochim. Acta* **1991**, *36*, 1485.

[33] K. Sugiura, S. Mikami, M. T. Johnson, J. W. Raebiger, J. S. Miller, K. Iwasaki, Y. Okada, S. Hinoc, Y. Sakata, *J. Mater. Chem.* **2001**, *11*, 2152.
[34] B. J. Tan, K. J. Klabunde, P. M. A. Sherwood, *J. Am. Chem. Soc.* **1991**, *113*, 855.
[35] A. Yoshino, T. Miyagi, E. Asato, M. Mikuriya, Y. Sakata, K. Sugiura, K. Iwasaki, S. Hino, *Chem. Commun.* **2000**, 1475.
[36] X. H. Bu, W. Chen, L. J. Mu, Z. H. Zhang, R. H. Zhang, T. Clifford, *Polyhedron* **2000a**, *19*, 2095.
[37] X. H. Bu, W. Chen, L. J. Mu, Z. H. Zhang, R. H. Zhang, T. Clifford, *Inorg. Chim. Acta* **2000b**, *310*, 110.
[38] R. Dhillon, S. F. Lincoln, S. Madbak, A. K. W. Stephens, K. P. Wainwright, S. L. Whitbread, *Inorg. Chem.* **2000**, *39*, 1855.
[39] R. Custelcean, M. Vlassa, J. E. Jackson, *Chem. -Eur. J.* **2002**, *8*, 302.
[40] P. J. Davies, S. F. Lincoln, C. B. Smith, M. R. Taylor, K. P. Wainwright, K. S. Wallwork, *Acta Crystallogr. C* **2000**, *56*, 28.
[41] R. D. Hancock, M. S. Shaikjee, S. M. Dobson, J. C. A. Boeyens, *Inorg. Chim. Acta* **1988a**, *154*, 229.
[42] R. Luckay, J. H. Reibenspies, R. D. Hancock, *Chem. Commun.* **1995**, 2365.
[43] X. D. Dong, X. Y. Wang, M. X. Lin, H. Sun, X. L. Yang, Z. J. Guo, *Inorg. Chem.* **2010**, *49*, 2541.
[44] J. Qian, W. Gu, H. Liu, F. X. Gao, L. Feng, S. P. Yan, D. Z. Liao, P. Cheng, *Dalton Trans.* **2007**, 1060.
[45] M. Cory, D. D. Mckee, J. Kagan, D. W. Henry, J. A. Miller, *J. Am. Chem. Soc.* **1985**, *107*, 2528.
[46] S. A. Tysoe, R. J. Morgan, A. D. Baker, T. C. Strekas, *J. Phys. Chem.* **1993**, *97*, 1707.
[47] J. Liu, T. X. Zhang, T. B. Lu, L. H. Qu, H. Zhou, Q. L. Zhang, L. N. Ji, *J. Inorg. Biochem.* **2002**, *91*, 269.
[48] B. M. Zeglis, V. C. Pierre, J. K. Barton, *Chem. Commun.* **2007a**, 4565.
[49] E. C. Long, J. K. Barton, *Acc. Chem. Res.* **1990**, *23*, 271.
[50] S. Kashanian, M. M. Khodaei, P. Pakravan, *DNA Cell Biol.* **2010**, *29*, 639.
[51] R. Indumathy, T. Weyhermüller, B. U. Nair, *Dalton Trans.* **2010b**, 2087.
[52] A. Hussain, S. Saha, R. Majumdar, R. R. Dighe, A. R. Chakravarty, *Dalton Trans.* **2010**, 1807.
[53] P. X. Xia, Z. H. Xu, F. J. Chen, Z. Z. Zeng, X. W. Zhang, *J. Inorg. Biochem.* **2009**, *103*, 210.
[54] B. Selvakumar, V. Rajendiran, P. Uma Maheswari, H. S. Evans, M. J. Palaniandavar, *J. Inorg. Biochem.* **2006**, *100*, 316.
[55] V. G. Vaidyanathan, B. U. Nair, *J. Inorg. Biochem.* **2003**, *94*, 121.
[56] H. Schneider, M. Wang, *J. Org. Chem.* **1994**, *59*, 7473.
[57] M. Roy, R. Santhanagopal, A. R. Chakravarty, *Dalton Trans.* **2009**, 1024.
[58] Q. Liu, J. Zhang, M. Q. Wang, D. W. Zhang, Q. S. Lu, Y. Huang, H. H. Lin, X. Q. Yu, *Eur. J. Med. Chem.* **2010**, *45*, 5302.
[59] B. C. Baguley, M. LeBret, *Biochemistry* **1984**, *23*, 937.
[60] J. R. Akowicz, G. Webber, *Biochemistry* **1973**, *12*, 4161.
[61] M. Chauhan, K. Banerjee, F. Arjmand, *Inorg. Chem.* **2007**, *46*, 3072.
[62] B. Norden, F. Tjerneld, *Biopolymers* **1982**, *21*, 1713.
[63] B. Ranjbar, P. Gill, *Chem. Biol. Drug Des.* **2009**, *74*, 101.
[64] P. Lincoln, E. Tuite, B. Norden, *J. Am. Chem. Soc.* **1997**, *119*, 1454.
[65] P. U. Maheswari, M. Palaniandavar, *J. Inorg. Biochem.* **2004**, *98*, 219.
[66] S. Mathur, S. Tabassum, *Biometals* **2008**, *21*, 299.
[67] Y. Shao, X. Sheng, Y. Li, Z. L. Jia, J. J. Zhang, F. Liu, G. Y. Lu, *Bioconjugate Chem.* **2008**, *19*, 1840.
[68] K. Karidi, A. Garoufis, N. Hadjiliadis, J. Reedijk, *Dalton Trans.* **2005**, 728.
[69] E. Gallori, C. Vettori, E. Alessio, F. G. Vilchez, R. Vilaplana, P. Orioli, A. Casini, L. Messori, *Arch. Biochem. Biophys.* **2000**, *376*, 156.
[70] K. M. Deck, T. A. Tseng, J. N. Burstyn, *Inorg. Chem.* **2002**, *41*, 669.
[71] C. Sissi, F. Mancin, M. Gatos, M. Palumbo, P. Tecilla, U. Tonellato, *Inorg. Chem.* **2005**, *44*, 2310.
[72] A. Sreedhara, J. D. Freed, J. A. Cowan, *J. Am. Chem. Soc.* **2000**, *122*, 8814.
[73] X. Sheng, X. M. Lu, J. J. Zhang, Y. T. Chen, G. Y. Lu, Y. Shao, F. Liu, Q. Xu, *J. Org. Chem.* **2007**, *72*, 1799.
[74] J. Tan, B. C. Wang, L. C. Zhu, *J. Biol. Inorg. Chem.* **2009**, *14*, 727.
[75] C. Bailly, J. B. Chaires, *Bioconjugate Chem.* **1998**, *9*, 513.
[76] A. De, V. Ramesh, S. Mahadevan, V. Nagaraja, *Biochemistry* **1998**, *37*, 3831.
[77] B. N. Conner, T. Takano, S. Tanaka, K. Italkura, R. E. Dickerson, *Nature* **1982**, *295*, 294.
[78] R. M. Hartshorn, J. K. Barton, *J. Am. Chem. Soc.* **1992**, *114*, 5919.
[79] B. P. Hudson, J. K. Barton, *J. Am. Chem. Soc.* **1998**, *120*, 6877.
[80] B. M. Zeglis, V. C. Pierre, J. K. Barton, *Chem. Commun.* **2007b**, 4565.
[81] A. K. Patra, T. Bhowmick, S. Ramakumar, M. Nethajia, A. R. Chakravarty, *Dalton Trans.* **2008**, 6966.
[82] T. Gupta, S. Dhar, M. Nethaji, A. R. Chakravarty, *Dalton Trans.* **2004**, 1896.
[83] A. K. Patra, M. Nethaji, A. R. Chakravarty, *J. Inorg. Biochem.* **2007**, *101*, 233.
[84] S. Satyanarayana, J. C. Dabrowiak, J. B. Chaires, *Biochemistry* **1992**, *31*, 9319.
[85] C. W. Garvie, C. Wolberger, *Mol. Cell* **2001**, *8*, 937.
[86] R. D. Hancock, M. S. Shaikjee, S. M. Dobson, J. C. A. Boeyens, *Inorg. Chim. Acta* **1988b**, *154*, 229.
[87] H. Mamela, R. D. Hancock, L. Carlton, J. H. Reibenspies, K. P. Wainwright, *J. Am. Chem. Soc.* **1995**, *117*, 6698.
[88] K. O. A. Chin, J. R. Morrow, C. H. Lake, M. R. Churchill, *Inorg. Chem.* **1994**, *33*, 656.
[89] G. M. Sheldrick, SADABS, Program for area detector adsorption correction, Institute for Inorganic Chemistry, University of Göttingen, Germany, **1996**.
[90] G. M. Sheldrick, *Acta Crystallogr. A* **2008**, *64*, 112.
[91] J. Marmur, *J. Mol. Biol.* **1961**, *3*, 208.
[92] M. E. Reichmann, S. A. Rice, C. A. Thomas, P. Doty, *J. Am. Chem. Soc.* **1954**, *76*, 3047.
[93] S. Satyanarayana, J. C. Dabrowiak, J. B. Chaires, *Biochemistry* **1993**, *32*, 2573.